Zeeman-type energy level splittings controlled by an electric field

Hong Jian Zhao,[1,2] Yanchao Wang,[1,3,*] Yurong Yang,[4] Yanming Ma,[1,3,5,†] and Laurent Bellaiche[6]

[1]*International Center for Computational Method and Software, College of Physics, Jilin University, Changchun 130012, China*

[2]*Key Laboratory of Physics and Technology for Advanced Batteries (Ministry of Education), College of Physics, Jilin University, Changchun 130012, China*

[3]*State Key Laboratory of Superhard Materials, College of Physics, Jilin University, Changchun 130012, China*

[4]*Department of Materials Science and Engineering, National Laboratory of Solid State Microstructures, Jiangsu Key Laboratory of Artificial Functional Materials, Nanjing University, Nanjing 210093, China*

[5]*International Center of Future Science, Jilin University, Changchun 130012, China*

[6]*Physics Department, Institute for Nanoscience and Engineering, University of Arkansas, Fayetteville, Arkansas 72701, USA*

(Received 25 January 2022; revised 6 June 2022; accepted 22 June 2022; published 6 July 2022)

Two-level systems are at the heart of quantum information and quantum computation based on qubits. The manipulation of Zeeman-type energy-level splittings is crucial for utilizing two-level systems hosted by electronic spin or pseudospin in crystalline materials. Of particular interest are Zeeman-type energy level splittings controlled by the electric field, most of which were realized in materials involving both spin and nonspin degrees of freedom that are entangled strongly via spin-orbital interaction. Here, we provide a strategy enabling the electric-field control of Zeeman-type energy-level splitting rooted in the nonspin degree of freedom of electrons—essentially from sublattice/atomic orbitals—in materials containing nonsymmorphic symmetry elements (e.g., glide plane or screw axis). The physical origin of such a Zeeman-type splitting is revealed as the breakdown of the specific nonsymmorphic symmetry elements by electric field. We further propose, via first-principles simulations, a platform system of $CaTiO_3$ under tensile strain (ferroelectric compound) that accommodates a large Zeeman-type energy-level splitting of ∼124 meV, controllable by the electric field.

DOI: 10.1103/PhysRevB.106.024104

I. INTRODUCTION

The qubits, represented by two-level systems, is at the core position of quantum information and quantum computation [1]. The electronic spin or pseudospin (see, e.g., Ref. [2] for the notion of pseudospin) degree of freedom (DOF) is an ideal platform for such two-level systems [3]. The basic conditions for utilizing the (pseudo)spin DOF in materials require: (i) that Zeeman-type splittings of electronic (pseudo)spin energy levels exist, and (ii) that such Zeeman-type splittings can be controlled [4,5]. Of particular interest is the coherent manipulation of spin or pseudospin Zeeman splittings by the electric field. Regarding electronic spin, the Zeeman-type splittings manipulated by the electric field have already been realized in WSe_2 [6] and two-dimensional hole systems [7]. Besides, valley, the local maxima or minima of electronic band energy of solids [8], constitutes a two-level pseudospin system [3]. Strikingly, the electric control of valley Zeeman splitting was also achieved in, e.g., the heterostructures formed by bilayer graphene/WSe_2 [9,10], and $CuInP_2S_6/MnPS_3$ [8].

Most of the electrically controllable Zeeman-type (pseudo)spin splittings are microscopically ascribed to spin-orbital interaction (SOI) involving both electronic spin and nonspin DOFs [11] with the following dilemma. Usually, large SOI is beneficial for creating the giant Zeeman splitting, in favor of distinguishing the two (pseudo)spin states. However, large SOI will entangle spin and nonspin DOFs strongly, leading to the decoherence of the (pseudo)spin system and reducing the lifetime of (pseudo)spin states [4,12]. A possible avenue to circumvent this dilemma may be by getting rid of electronic spin and employing electronic nonspin DOF to achieve Zeeman-type energy level splitting.

Here, we report a general scheme to realize Zeeman-type energy level splittings which only involve electronic nonspin DOF and are controllable by the electric field. In crystals with nonsymmorphic symmetry elements (e.g., glide plane or screw axis), the nonspin DOFs of electrons may form a two-level system in the absence of SOI. Through symmetry analysis, we demonstrate that electric field can lift the band degeneracy and cause Zeeman-type energy level splittings by breaking the specific nonsymmorphic symmetry elements. Based on first-principles calculations, we propose the tensilely strained $CaTiO_3$ film as a possible candidate showcasing a large Zeeman-type energy level splitting of ∼124 meV, that is controllable by the electric field.

II. RESULTS

A. Strategy towards our proposed two-level system

First, let us recall that the electronic energy levels in materials are generally linked with both spin and nonspin DOFs

*wyc@calypso.cn
†mym@jlu.edu.cn

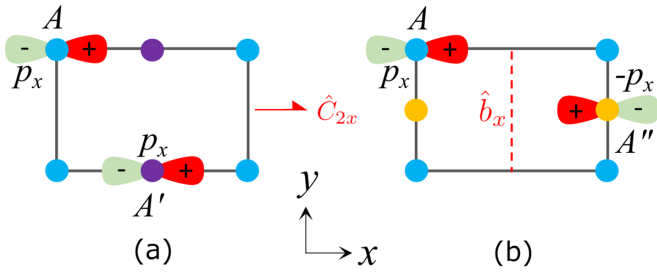

FIG. 1. Sketches of crystals with (a) nonsymmorphic screw axis $\hat{C}_{2x}$ and (b) glide plane $\hat{b}_x$. The two-dimensional crystals incorporating A and A' (A'') sublattices are taken as examples. The lattice vectors of the crystals parallel to x and y orientations are denoted by **a** and **b**, respectively. The $\hat{C}_{2x}$ symmetry operation first rotates the system around the twofold axis (red arrow in panel a) then translates it by $\frac{1}{2}$**a**. The glide plane $\hat{b}_x$ transforms the crystal by a mirror plane (red dashed line in panel b) followed by a lattice translation of $\frac{1}{2}$**b**.

(see, e.g., Refs. [13–16]). Materials with large SOI or magnetism may present dominant spin splitting, the splitting of electronic spin energy levels. On the contrary, the spin splitting in nonmagnetic materials with negligible SOI is expected to be either null or too tiny to detect. Therefore, the energy level splitting in such materials is nearly related to nonspin energy levels. [Note that as a counterpart of spin, nonspin DOFs in solids were recently found to present some intriguing features, such as orbital magnetism (see, e.g., Refs. [17,18])]. In the present paper, we aim at realizing a two-level system, contributed by nonspin DOF, in nonmagnetic materials without the inclusion of large SOI.

Next, we explore the possibility to create and manipulate this two-level system. In crystals with nonsymmorphic space groups, there are several sublattices containing the same atomic species. Those sublattices together with the corresponding sublattice orbitals are "connected" with each other by nonsymmorphic symmetry operations, such as screw axes and glide planes [19]. For example, as sketched in Fig. 1, the twofold screw axis (respectively, glide plane) establishes the correlation between A and A' (respectively, A'') sublattices. Consequently, the p_x orbital of A is, according to symmetry, related with the p_x orbital of A' by $\hat{C}_{2x}$, and with the $-p_x$ orbital of A'' by $\hat{b}_x$, respectively (Fig. 1). This implies the additional band degeneracy at a specific **k** point in the Brillouin zone of a nonsymmorphic space group as suggested by a group theory textbook [19] together with several previous studies (see, e.g., Refs. [13–16]). If the degeneracy is twofold, a two-level system will naturally be prepared. Now, we should find an approach to create and manipulate the Zeeman-type energy level splitting in this two-level system. To this end, an electric field may be applied to the material for breaking its nonsymmorphic symmetry operations. Such symmetry breaking probably lifts the twofold band degeneracy by cutting off the correlation between various sublattice orbitals in the material.

In the following, we will do symmetry analysis to testify our strategy, taking the nonmagnetic *Pbnm* space group as a platform. The reason why we employ *Pbnm* is that such a space group is very common in materials, for example, more than half of the perovskites adopt such symmetry [20].

TABLE I. The symmetry-protected band degeneracy at various **k** points for *Pbnm*, $P2_1nm$, $Pb2_1m$, and $Pbn2_1$ phases. The numbers "1" and "2" in the table denote the band degeneracy for the spinless case (i.e., without SOI) at that **k** point. The γ_i ($i = x, y, z$) matrix has the same form as the Pauli matrix σ_i. The splitting terms are with respect to the *Pbnm* space group.

	Pbnm	$P2_1nm$	$Pb2_1m$	$Pbn2_1$	Splitting terms
$X(\frac{1}{2}, 0, 0)$	2	2	1	2	$k_x\gamma_y, E_y\gamma_x$
$Y(0, \frac{1}{2}, 0)$	2	1	2	2	$k_y\gamma_y, E_x\gamma_x$
$Z(0, 0, \frac{1}{2})$	2	2	1	2	$k_z\gamma_y, E_y\gamma_x$
$U(\frac{1}{2}, 0, \frac{1}{2})$	2	2	1	2	$E_y\gamma_x$

In particular, we do not include the SOI—the spin-up and spin-down electrons are, thus, indistinguishable—so that our Zeeman-type energy level splittings mentioned below involve only nonspin DOFs.

B. Symmetry analysis

As shown in Sec. I of the Supplemental Material (SM) [21] (also including Refs. [22–53]), the *Pbnm* space group contains the following nonsymmorphic symmetry operations: screw axes $\hat{C}_{2x}, \hat{C}_{2y}, \hat{C}_{2z}$, and glide planes $\hat{b}_x, \hat{n}_y$. Consequently, the high-symmetric R, S, T, X, Y, Z, and U points in the Brillouin zone of the *Pbnm* space group exhibit additional band degeneracy, which is demonstrated in Tables S2 and S3 of the SM [21]. Such band degeneracies may be destroyed when polarizing *Pbnm* materials along the x, y, or z direction. For instance, the X point is twofold degenerate for *Pbnm* as a consequence of screw axis $\hat{C}_{2x}$ or glide plane $\hat{n}_y$ (see Table S3 of the SM [21]), realizing a two-level system. Applying electric-field E_y (i.e., along the y direction) to *Pbnm* material will transform it into the $Pb2_1m$ space group, which contains $\hat{C}_{2y}$ and $\hat{b}_x$ nonsymmorphic symmetry operations instead. Without the symmetry protection provided by $\hat{C}_{2x}$ or $\hat{n}_y$, the degenerate energy levels at the X point is split into nondegenerate ones, ratifying the Zeeman-type energy level splitting. Using this logic and according to Table S3 of the SM [21], the symmetry-enforced energy level degeneracy at X, Y, Z, and U points for *Pbnm*, $P2_1nm$, $Pb2_1m$, and $Pbn2_1$ are summarized in Table I and sketched in Fig. 2. We, thus, based on symmetry analysis, conclude that: (i) applying electric-field E_x to *Pbnm* or $Pb2_1m$ can drive the system to $P2_1nm$ symmetry, leading to the Zeeman-type splittings around the Y point [from Figs. 2(a) or 2(e) to 2(b)]; (ii) electric-field E_y induces the Zeeman-type splittings around the X, Z, and U points, by driving the system from *Pbnm* or $P2_1nm$ to $Pb2_1m$ [from Figs. 2(a) or 2(c) to 2(d)]; and (iii) polarizing *Pbnm* along the z direction will not, on the other hand, create Zeeman-type splittings at the X, Y, Z, or U point. Furthermore, the electric field may also split the energy levels at R, S, and T points. However, even though the materials are polarized to the $P2_1nm$, $Pb2_1m$, or $Pbn2_1$ space group, the bands at R, S, and T points are, at least, twofold degenerate. That is, the electric field cannot fully split the bands at the R, S, or T point. The band structures around these three **k** points are, thus, not of interest and will not be discussed in the following text.

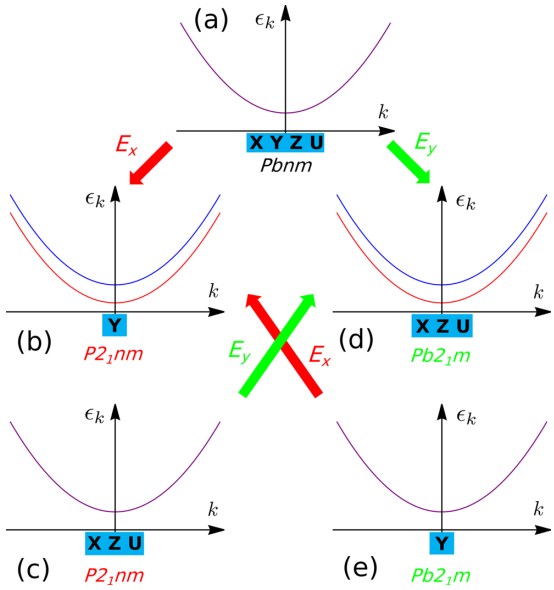

FIG. 2. Sketches of the band dispersion, around the X, Y, Z, and U points, for materials with $Pbnm$, $P2_1nm$, and $Pb2_1m$ space groups.

C. Model analysis

Moving away from the high-symmetric X, Y, Z, or U point possibly lowers the symmetry of the **k** point, giving rise to additional band splittings. To describe the band structures around the X, Y, Z, and U points, a straightforward way is to construct the two-band effective $k \cdot p$ Hamiltonian. As shown in Table I, we use the 2×2 matrix γ_i $(i = x, y, z)$ to capture the nonspin DOF of electrons in the $Pbnm$ space group since the band degeneracy at these **k** points is at most twofold. The band splitting terms up to first order in **k** are summarized in Table I. Let us concentrate first on the U point with the Zeeman-type splitting term given by $\xi E_y \gamma_x$ (ξ being a coefficient). Two eigenvalues $-\xi E_y$ and ξE_y result from such a term with their eigenstates denoted by $\psi_\uparrow$ and $\psi_\downarrow$, respectively. Here, $\psi_\uparrow$ and $\psi_\downarrow$ states span a two-dimensional Hilbert space that bears resemblance with the spin-$\frac{1}{2}$ electron. When switching the electric field to $-E_y$, the two eigenenergies are still $-\xi E_y$ and ξE_y but now associated with $\psi_\downarrow$ and $\psi_\uparrow$ states, respectively. This is similar to the Zeeman spin splitting $B_i\sigma_i$—appearing in materials under magnetic-field B_i $(i = x, y, z)$, where σ_i is the i component of the Pauli matrix [54]. We coin here this type of splitting as the Zeeman-type energy level splitting of the first kind. Similarly, a first kind Zeeman-type splitting also occurs around the X (along k_y and k_z), Y (along k_x and k_z), and Z (along k_x and k_y) points, as driven by the $E_y\gamma_x$ or $E_x\gamma_x$ splitting terms. Furthermore, there are also band splittings (i.e., $k_x\gamma_y$, $k_y\gamma_y$, or $k_z\gamma_y$) without involving the electric field when k is away from X, Y, or Z points. We call these splittings the Rashba/Dresselhaus-type energy level splittings since they are reminiscent of the linear Rashba/Dresselhaus spin splittings [55,56] in noncentrosymmetric semiconductors. In the presence of electric field E_x or E_y, the Zeeman-type energy level splittings (e.g., $E_y\gamma_x$ or $E_x\gamma_x$) can be superimposed on the Rashba-/Dresselhaus-type energy level splittings (e.g., $k_i\gamma_y$, $i = x, y, z$). Such a mixture of Zeeman-type and Rashba-/Dresselhaus-type splittings is denoted here as the Zeeman-type energy level splitting of the second kind.

Furthermore, our models can readily be generalized to ferroelectric phases with $P2_1nm$ or $Pb2_1m$ symmetry, if we interpret electric field E_x or E_y as electric polarization P_x or P_y, respectively. For instance, the Zeeman-type splitting term around the U point for the $Pb2_1m$ phase now reads $\xi P_y \gamma_x$. Switching the polarization by electric field, therefore, manipulates the two-level states. As shown in Figs. 2(b)–2(e), switching from $P2_1nm$ to $Pb2_1m$ (respectively, from $Pb2_1m$ to $P2_1nm$) leads to the first or second kind of Zeeman-type energy level splittings around the X, Z, and U points (respectively, Y point). Such features allow an interesting avenue towards the nonvolatile ferroelectric manipulation of Zeeman-type energy level splittings in ferroelectrics adopting both $Pb2_1m$ and $P2_1nm$ phases. By the wording nonvolatile, we mean that the energy band status created by the electric field can be persistent even when the electric field is removed.

D. Strained $CaTiO_3$ film as a candidate

We next propose a real material not only to corroborate our aforementioned symmetry and model analysis, but also to provide opportunities (e.g., material support) for the design of devices utilizing the electric control of Zeeman-type energy level splitting. We select the nonmagnetic perovskite $CaTiO_3$ material as our test bed. In particular, $CaTiO_3$ does not contain elements with large atomic numbers, and the SOI is, therefore, expected to be weak. Promisingly, at some tensile strains, the epitaxial $CaTiO_3$ thin film was predicted to be a ferroelectric semiconductor with a $P2_1nm$ ground state and a $Pb2_1m$ metastable phase [57]. Our SM [21] provides results of first-principles simulations that basically reproduce the findings of Ref. [57] (see Sec. III.1 of the SM [21]). We also predict that an electric-field E_y of $\sim$2.9 MV/cm will induce a transition from $P2_1nm$ to $Pb2_1m$, whereas an E_x of $\sim$2.0 MV/cm will generate the backwards transition (see Sec. III.2 of the SM [21]). Using the first-principles technique, we further compute the local band structures around the U, X, Y, and Z points, along k_x, k_y, and k_z directions. In particular, we select two bands in the vicinity of the valence-band maximum for analysis as shown in Fig. 3 of the Main Text and Fig. S4 of the SM [21]. Our $k \cdot p$ models, incorporating the effective mass terms, band splitting terms, and higher-order-in-k corrections (see Sec. II of the SM [21]), reproduce the first-principles band structures quite well at small k. In particular, around the U point, the bands are twofold degenerate along the k_x, k_y, and k_z directions in the $P2_1nm$ phase as consistent with our aforementioned symmetry analysis. When switching to the $Pb2_1m$ phase (by, e.g., applying E_y), the first-kind Zeeman-type energy level splittings occur around the U point as correctly predicted by our model with the splitting magnitude being about 124 meV. Such a splitting is comparable to the spin splitting value in, e.g., diluted magnetic semiconductors $Zn_{0.95}Mn_{0.05}Te$, in the presence of a magnetic field of $\sim$10 T [58]. Finally, the Zeeman-type energy level splittings around the X, Y, and Z points are also confirmed by our first-principles calculations and are discussed in details in Sec. III.3 of the SM [21]. In particular, when transiting the phase $Pb2_1m$ back to $P2_1nm$, (by, e.g., the application of E_x), the first-kind

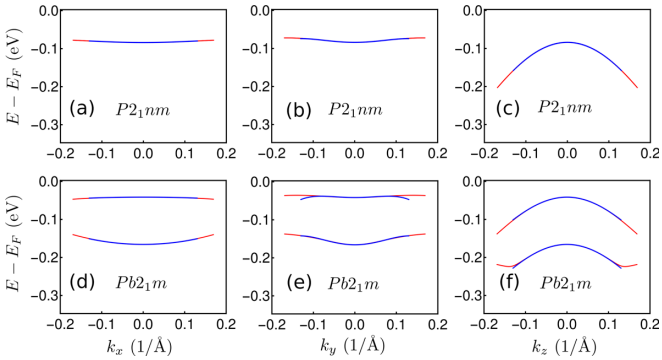

FIG. 3. The local band structures of $P2_1nm$ and $Pb2_1m$ phases of $CaTiO_3$ around the U point. The band structures calculated by first-principles and fitted by our model are shown as red lines and blue lines, respectively. The Fermi-level E_F is set as the valence-band maximum.

Zeeman-type energy level splittings appear along the k_x and k_z directions, whereas the second-kind Zeeman-type splitting happens along k_y (see Fig. S4 of the SM [21]) both around the Y point, once again consistent with our symmetry analysis provided above.

III. OUTLOOK

So far, we have proposed a mechanism to achieve in nonsymmorphic space groups a two-level system, which is spanned by electronic nonspin DOFs. In particular, our analysis reveals the crucial role of breaking the nonymmorphic symmetry elements (by electric field) towards the electrically controllable Zeeman-type energy level splitting. As a result, we can generalize our approach to the 157 nonsymmorphic space groups known in condensed matter. Our proposal, therefore, offers a wide spectrum of materials to select for designing devices based on electronic nonspin DOFs. For example, researchers may employ the Materials Project [41] or the ICSD [59] databases to select the already-synthesized materials with nonsymmorphic space groups for such a design. Other compounds with nonsymmorphic space groups and electric-field-driven Zeeman-type energy level splittings can also be predicted by structural prediction techniques [60], such as CALYPSO [61].

ACKNOWLEDGMENTS

This research was supported by the Natural Science Foundation of China (Grants No. 12034009, No. 12174142, No. 11974134, and No. 91961204). L.B. acknowledges the Vannevar Bush Faculty Fellowship (VBFF) Grant No. N00014-20-1-2834 from the Department of Defense and the MonArk Quantum Foundry supported by the National Science Foundation Q-AMASE-i program under NSF Award No. DMR-1906383. We acknowledge the support from Jilin Province Science and Technology Development Program (Grant No. YDZJ202102CXJD016), Program for Jilin University Science and Technology Innovative Research Team, and Program for Jilin University Computational Interdiscipline Innovative Platform. We are also thankful for the computational support from the Arkansas High Performance Computing Center (AHPCC). We thank Prof. S. Yang, Prof. W. Mi, and Prof. L. Tao for valuable discussions on time-reversal symmetry.

[1] C. H. Bennett and D. P. DiVincenzo, Nature (London) **404**, 247 (2000).
[2] A. Manchon, H. C. Koo, J. Nitta, S. M. Frolov, and R. A. Duine, Nature Mater. **14**, 871 (2015).
[3] X. Xu, W. Yao, D. Xiao, and T. F. Heinz, Nat. Phys. **10**, 343 (2014).
[4] T. Schäpers, *Semiconductor Spintronics* (De Gruyter, Berlin, 2016).
[5] Z. Ye, D. Sun, and T. F. Heinz, Nat. Phys. **13**, 26 (2017).
[6] H. Yuan, M. S. Bahramy, K. Morimoto, S. Wu, K. Nomura, B.-J. Yang, H. Shimotani, R. Suzuki, M. Toh, C. Kloc, X. Xu, R. Arita, N. Nagaosa, and Y. Iwasa, Nat. Phys. **9**, 563 (2013).
[7] E. Marcellina, A. Srinivasan, D. S. Miserev, A. F. Croxall, D. A. Ritchie, I. Farrer, O. P. Sushkov, D. Culcer, and A. R. Hamilton, Phys. Rev. Lett. **121**, 077701 (2018).
[8] H. Hu, W.-Y. Tong, Y.-H. Shen, and C.-G. Duan, J. Mater. Chem. C **8**, 8098 (2020).
[9] J. Ingla-Aynés, F. Herling, J. Fabian, L. E. Hueso, and F. Casanova, Phys. Rev. Lett. **127**, 047202 (2021).
[10] P. Tiwari, S. K. Srivastav, and A. Bid, Phys. Rev. Lett. **126**, 096801 (2021).
[11] Here, the spatial (i.e., nonspin) parts of electronic quantum states, such as atomic orbital and sublattice orbital degrees of freedom, are collectively referred to as electronic nonspin degree of freedom.
[12] J. Fabian, A. Matos-Abiague, C. Ertler, P. Stano, and I. Zutic, Acta Phys. Slovaca **57**, 565 (2007).
[13] L. L. Tao, T. R. Paudel, A. A. Kovalev, and E. Y. Tsymbal, Phys. Rev. B **95**, 245141 (2017).
[14] L. L. Tao and E. Y. Tsymbal, Nat. Commun. **9**, 2763 (2018).
[15] L. Yuan, Q. Liu, X. Z. Zhang, J.-W. Luo, S.-S. Li, and A. Zunger, Nat. Commun. **10**, 906 (2019).
[16] H. J. Zhao, P. Chen, C. Paillard, R. Arras, Y.-W. Fang, X. Li, J. Gosteau, Y. Yang, and L. Bellaiche, Phys. Rev. B **102**, 041203(R) (2020).
[17] D. Go, J.-P. Hanke, P. M. Buhl, F. Freimuth, G. Bihlmayer, H.-W. Lee, Y. Mokrousov, and S. Blügel, Sci. Rep. **7**, 46742 (2017).
[18] J. H. Ryoo and C.-H. Park, NPG Asia Mater. **9**, e382 (2017).
[19] M. S. Dresselhaus, G. Dresselhaus, and A. Jorio, *Group Theory: Application to the Physics of Condensed Matter* (Springer-Verlag, Berlin Heidelberg, 2008).
[20] M. W. Lufaso and P. M. Woodward, Acta Crystallogr., Sect. B: Struct. Sci. **57**, 725 (2001).
[21] See Supplemental Material at http://link.aps.org/supplemental/10.1103/PhysRevB.106.024104 for symmetry analysis, methods, and some numerical results (phase transitions in $CaTiO_3$

induced by strain, electric field, and band structures around several high-symmetry k points for ferroelectric $P2_1nm$ and $Pb2_1m$ $CaTiO_3$).
[22] J. K. Asbóth, L. Oroszlány, and A. Pályi, *A Short Course on Topological Insulators: Band Structure and Edge States in One and Two Dimensions* (Springer, Cham, 2016).
[23] S. M. Young and C. L. Kane, Phys. Rev. Lett. **115**, 126803 (2015).
[24] G. Kresse and J. Furthmüller, Phys. Rev. B **54**, 11169 (1996).
[25] G. Kresse and D. Joubert, Phys. Rev. B **59**, 1758 (1999).
[26] G. I. Csonka, J. P. Perdew, A. Ruzsinszky, P. H. T. Philipsen, S. Lebègue, J. Paier, O. A. Vydrov, and J. G. Ángyán, Phys. Rev. B **79**, 155107 (2009).
[27] P. E. Blöchl, Phys. Rev. B **50**, 17953 (1994).
[28] M. I. Aroyo, A. Kirov, C. Capillas, J. M. Perez-Mato, and H. Wondratschek, Acta Crystallogr., Sect. A: Found Crystallogr. **62**, 115 (2006).
[29] M. I. Aroyo, J. M. Perez-Mato, C. Capillas, E. Kroumova, S. Ivantchev, G. Madariaga, A. Kirov, and H. Wondratschek, Z. Kristallogr.-Cryst. Mater. **221**, 15 (2006).
[30] "Generators of space groups," https://www.cryst.ehu.es/cryst/get_gen.html
[31] "Irreducible representations of the space groups," https://www.cryst.ehu.es/cgi-bin/cryst/programs/representations.pl?tipogrupo=spg
[32] "Point group tables," https://www.cryst.ehu.es/rep/point.html
[33] "Isotropy software suite," https://stokes.byu.edu/iso/isotropy.php
[34] H. T. Stokes and D. M. Hatch, J. Appl. Crystallogr. **38**, 237 (2005).
[35] "Findsym," https://stokes.byu.edu/iso/findsym.php
[36] "Seek-path," https://www.materialscloud.org/work/tools/seekpath
[37] Y. Hinuma, G. Pizzi, Y. Kumagai, F. Oba, and I. Tanaka, Comput. Mater. Sci. **128**, 140 (2017).
[38] A. Togo and I. Tanaka, `Spglib`: a software library for crystal symmetry search, arXiv:1808.01590.
[39] "Pymatgen," https://pymatgen.org/
[40] S. P. Ong, W. D. Richards, A. Jain, G. Hautier, M. Kocher, S. Cholia, D. Gunter, V. L. Chevrier, K. A. Persson, and G. Ceder, Comput. Mater. Sci. **68**, 314 (2013).
[41] "Materials project," https://materialsproject.org/
[42] A. Jain, S. P. Ong, G. Hautier, W. Chen, W. D. Richards, S. Dacek, S. Cholia, D. Gunter, D. Skinner, G. Ceder, and K. A. Persson, APL Mater. **1**, 011002 (2013).
[43] W. R. Inc., "*Mathematica*, Version 12.0," Champaign, IL, 2019.
[44] K. Momma and F. Izumi, J. Appl. Crystalallogr. **44**, 1272 (2011).
[45] V. Wang, N. Xu, J.-C. Liu, G. Tang, and W.-T. Geng, Comput. Phys. Commun. **267**, 108033 (2021).
[46] "Vaspkit," https://vaspkit.com/
[47] J. D. Hunter, Comput. Sci. Eng. **9**, 90 (2007).
[48] R. D. King-Smith and D. Vanderbilt, Phys. Rev. B **47**, 1651 (1993).
[49] G. Henkelman and H. Jónsson, J. Chem. Phys. **113**, 9901 (2000).
[50] G. Henkelman and H. Jónsson, J. Chem. Phys. **113**, 9978 (2000).
[51] "Transition state tools for vasp," https://theory.cm.utexas.edu/vtsttools/index.html
[52] H. Fu and L. Bellaiche, Phys. Rev. Lett. **91**, 057601 (2003).
[53] H. J. Zhao, H. Nakamura, R. Arras, C. Paillard, P. Chen, J. Gosteau, X. Li, Y. Yang, and L. Bellaiche, Phys. Rev. Lett. **125**, 216405 (2020).
[54] Consequently, our proposed Zeeman-type energy level splitting can be seen as a kind of pseudospin splittings.
[55] Y. A. Bychkov and E. I. Rashba, JETP Lett. **39**, 78 (1984).
[56] G. Dresselhaus, Phys. Rev. **100**, 580 (1955).
[57] C.-J. Eklund, C. J. Fennie, and K. M. Rabe, Phys. Rev. B **79**, 220101(R) (2009).
[58] R. L. Aggarwal, S. N. Jasperson, P. Becla, and J. K. Furdyna, Phys. Rev. B **34**, 5894 (1986).
[59] "Icsd," https://icsd.products.fiz-karlsruhe.de/
[60] L. Zhang, Y. Wang, J. Lv, and Y. Ma, Nat. Rev. Mater. **2**, 17005 (2017).
[61] "Calypso," http://www.calypso.cn/